J Ther Eng, Vol. 11, No. 4, pp. 1011–1023, July, 2025

Journal of Thermal Engineering
Web page info: https://jten.yildiz.edu.tr
DOI: 10.14744/thermal.0000960

Research Article

Temperature evolution within a solar panel using a cooling source of varying sizes and shapes in the presence of a hybrid nanofluid

Boubekeur GHAZI[1,*], **Syham KADRI**[1,2,*], **Razli MEHDAOUI**[1,3]

[1]ENERGARID Laboratory, Tahri Mohamed University, Bechar, 08000, Algeria
[2]LPDS Laboratory, Tahri Mohamed University, Bechar, 08000, Algeria
[3]L2ME Laboratory, Tahri Mohamed University, Bechar, 08000, Algeria

ARTICLE INFO

Article history
Received: 23 May 2024
Revised: 24 August 2024
Accepted: 24 August 2024

Keywords:
Hybrid Nanofluid; Circular Cold Cylinder; Square Cold Cylinder; Temperature Solar Panel; Natural Convection; Finite Element Method; Triangular Cavity

ABSTRACT

A triangle space with a submerged cold cylinder of varying sizes and shapes is the subject of this computational investigation of spontaneous thermal convection. The (Al_2O_3-Cu-water) hybrid nanofluid fills the triangle space using an aspect ratio and the geometry of the cold source immersed in the solar panel. The objective of this project is to enhance the performance of the panel by increasing the evacuation rate of convective heat transfer. The second goal is to conduct digital research that will enable a reliable selection of data for the panel future design. Therefore, this work has significance since it allows for lowering the temperature and boosting the solar panel efficiency despite the challenging conditions in our dry border region (south-west Algeria). With a Rayleigh number of 10^6 and based on information from our dry location (southwest Algeria), with the solar panel angled at 30°, we tested three distinct cases: one with S_L=0.04, another with S_L=0.06 and the last one with S_L= 0.08. The coupling of the flow-governing equations in our investigation is solved by a quadratic Lagrange interpolation utilizing the finite element approach. Following the establishment of the optimal dimension, five distinct shapes of the cold source are examined to ascertain the best shape for the evacuation of convective heat transfer within a triangle cavity. Temperature profiles, average Nusselt number, streamline and isotherm patterns are all part of the collected data. Based on the findings of this experiment, the convective transfer mode can only be dominant when the source is circular with a diameter of S_L= 0.08. Near the source, it has been found that the temperature of the solar panel is reduced, which is a significant result. There is a strong agreement when we compare the average Nusselt number of our code to that of Keramat.

Cite this article as: Ghazi B, Kadri S, Mehdaoui R. Temperature evolution within a solar panel using a cooling source of varying sizes and shapes in the presence of a hybrid nanofluid. J Ther Eng 2025;11(4):1011–1023.

***Corresponding author.**
*E-mail address: kadri.syham@univ-bechar.dz

This paper was recommended for publication in revised form by Editor-in-Chief Ahmet Selim Dalkılıç

Published by Yıldız Technical University Press, İstanbul, Turkey

INTRODUCTION

The field of heat transfer is a significant focus of this study. Hybrid nanofluids, known for their superior thermal conductivity compared to conventional fluids, are gaining prominence in this area. This research provides valuable insights for engineers and researchers aiming to optimize cooling systems for electronic devices, such as solar panels [1]. The performance of solar panels in hot climates has been extensively studied [2-4]. Furthermore, investigations into laminar natural convection through various cavity shapes can enhance our understanding and improvement of various engineering applications, including solar collectors [5-7].

Free convective heat transfer is commonly utilized in electrical systems to provide efficient heat dissipation. Convective liquid metal cooling is one method; its special thermal characteristics provide excellent performance [8]. Recent developments in the electronic sector have raised interest in convective heat transfer in different limited enclosures with heat sources. Natural convection has been the subject of numerous investigations about heat transfer in cavities filled with nanofluids when a heat source is present [9–14]. The use of natural convection to transfer heat from a heat source to a nanofluid-filled cavity has been the subject of numerous studies. Various numerical techniques, including the finite volume method and the Boltzmann lattice method, were employed to solve heat transport via natural convection in the submitted work [15–17]. The natural convection of nanofluids has been experimentally examined by various researchers [18–20]. Researchers Rao et al. [21], P. M. Sankar et al. [22] and Dogonchi et al. [23] have also looked into the function of nanofluids in natural convection within porous containers. An emerging area of study, known as a "hybrid" nanofluid, is steadily expanding in tandem with the ever-expanding capabilities of conventional nanofluids. This sort of nanofluid is created by suspending many types of nanoparticles in a base fluid. Several industrial applications rely heavily on hybrid nanofluids and materials. These include heat transfer [24-31], renewable energy technology [32], chemical engineering [32], solar energy devices [33, 34] and heat exchangers [35]. A.M. Rashad [36] looked into the transmission of thermal energy through the convection of two nanoparticles (Al_2O_3-Cu) from a scientific perspective that was heated from below by a continuous heat flux contained in an enclosure in a magnetic field. He found that increasing the volume percentage of the hybrid nanofluid has a substantial effect when the natural convection is very minimal. In addition, as compared to conventional nanofluid, the hybrid nanofluid made of equal parts Cu and Al_2O_3 nanoparticles in a water-based fluid does not significantly improve the average Nusselt number. S. Manjunatha et al. [37] focused on thermal flow. Thermogravimetric and viscosity-dependent hybrid nanofluid boundary layer flows with improved heat transmission. Furthermore, the impact of the Laurentz force on the flow is taken into account. Significant discovery: when certain conditions are present, the thermal conductivity of hybrid nanofluids is higher than that of normal nanofluids. A reduction in the variable viscosity causes the boundary layer thickness of both normal and hybrid nanofluids to drop. Both conventional nanofluid and hybrid nanofluid flow and temperature are proportional to the volume fraction. A triangular annular hollow was filled with a hybrid nanofluid of Al_2O_3/Cu and water. Fatih Selimefendigil et al. [38] statistically investigated the cavity's free convection.

They discovered that the Nusselt number was improved with an increase in the Rayleigh number and an aperture ratio. The opening ratio's impact on heat transmission is amplified as the Rayleigh numbers rise. There is a straight line connecting the increase in average heat transfer and the volume fraction of solid nanoparticles; the more thermally conductive the solid, the steeper the hill on the linear curve. For their study, A.I. Alsabery et al. [39] used a vertically undulated surface cavity with a heat source block at the base to examine natural convection within the cavity. The method utilizes the use of a nanofluid that is a combination of water, copper, and aluminum oxide. The results indicate that the Nusselt number is proportional to the heat source's length. Also, compared to regular nanofluids and pure water, the Nusselt number of the water-Cu-Al_2O_3 hybrid is larger. Compared to pure water and other nanofluids, the hybrid nanofluid achieves average heat transfer percentages that are 13.7% and 5% greater, respectively, at $\varphi = 0.02$. The impact of impediments and their placement inside the square hole (L = H) on heat transfer is the primary subject of Farid Hachichi et al. [40]. Mixed nanofluid movement and heat exchange are greatly affected by the value of square barriers within the square-shaped cavity, according to the data. According to their findings, the hybrid nanofluid heat transmission is enhanced when the obstruction reaches Y = 0.25H.

In recent years, a number of research projects have made use of various geometries of enclosures housing heat sources [41-46]. The computational and empirical research on internal and external factors influencing natural convection in sealed spaces has been compiled in a bibliographical review by Pandey [47]. In this review, many forms were considered, including elliptical, square, and circular cylinders as internal bodies. To enhance the flow's hydrodynamic and thermal behavior, he outlined the many approaches taken in the literature. Additional research on natural convection using hybrid nanofluids can be found in the cited works [48-54].

The present work explores convective heat transport involving computational analysis with a tilted wall design and a nanofluid mixture (Al_2O_3-Cu/water). It is essential to determine the optimal cold source size and the fractions of copper and aluminum oxide nanoparticles to enhance convective heat transfer. Situated in a dry border region (southwest Algeria), the solar panel is efficiently cooled.

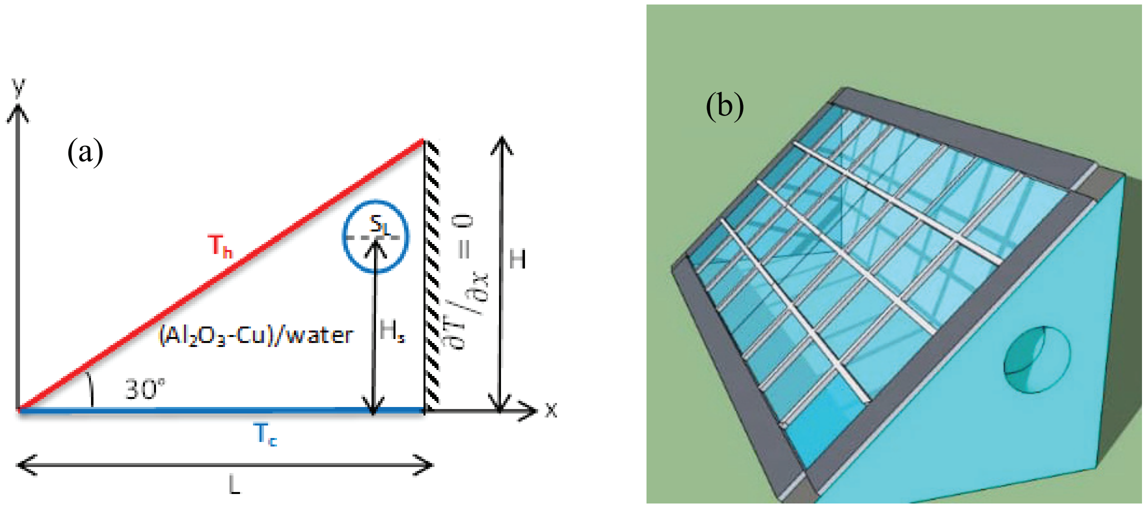

Figure 1. Physical Configuration: (a) 2D, (b) 3D.

PROBLEM AND THEORETICAL METHOD

The geometry that was investigated is shown in 2D in Figure 1(a) and in 3D in Figure 1(b). The major component is a mixed nanofluid made of water and (Al_2O_3-Cu) that flows across a triangle-shaped cavity with a height of H and a base of L. Our solar panel, which has dimensions of L_p=1.7m and H_p=1.15m, is heated by means of the slanted wall. Adiabatic describes the vertical wall. The temperature T_c of the cold generating cylinder and the horizontal wall remains constant. Assuming all physical properties, except density, which is represented using the Boussinesq approximation, are constant, Table 1 displays the Cu-Al_2O_3 mixed nanofluid physical attributes. Newtonian, homogeneous, incompressible, laminar, two-dimensional, stationary flow is presumed for the (Cu-Al_2O_3)-water hybrid nanofluid. The solar panel thickness is presumed to be insignificant.

The size of the cold source is mentioned by S_L (see Figure 1). The three cases studied are obtained by varying this dimension in: S_L=0.04 (case 1), S_L=0.06 (case 2) and S_L=0.08 (case 3).

The following is an example of a non-dimensional representation of the conservation equation that is reached by using the variables below [57]:

$$(x^*, y^*) = \frac{(x,y)}{L}\ ;(u^*, v^*) = \frac{(u,v)L}{\alpha f}\ ;T^* = \frac{(T-T_c)}{(T_h-T_c)}\ ;$$
$$P^* = \frac{PL^2}{\rho_{hnf}\alpha_f^2}$$

$$\frac{\partial u^*}{\partial x^*} + \frac{\partial v^*}{\partial y^*} = 0 \tag{1}$$

$$\rho_{hnf}\left[u^*\frac{\partial u^*}{\partial x^*} + v^*\frac{\partial v^*}{\partial y^*}\right] = -\frac{\partial P^*}{\partial x^*} + \frac{Pr}{(1-\varphi_1)^{2.5}(1-\varphi_2)^{2.5}}\left[\frac{\partial^2 u^*}{\partial x^{*2}} + \frac{\partial^2 u^*}{\partial y^{*2}}\right] \tag{2}$$

$$\rho_{hnf}\left[u^*\frac{\partial u^*}{\partial x^*} + v^*\frac{\partial v^*}{\partial y^*}\right] = -\frac{\partial P^*}{\partial y^*} + \frac{Pr}{(1-\varphi_1)^{2.5}(1-\varphi_2)^{2.5}}\left[\frac{\partial^2 v^*}{\partial x^{*2}} + \frac{\partial^2 v^*}{\partial y^{*2}}\right] + RaPr\beta_{hnf}T^* \tag{3}$$

$$u^*\frac{\partial T^*}{\partial x^*} + v^*\frac{\partial T^*}{\partial y^*} = \frac{\alpha_{hnf}}{\alpha_f}\left[\frac{\partial^2 T^*}{\partial x^{*2}} + \frac{\partial^2 T^*}{\partial y^{*2}}\right] \tag{4}$$

With T* representing the dimensionless temperature and P* the dimensionless pressure, with u* and v* denoting the x- and y-direction velocity components, respectively.

The Rayleigh number Ra and the Prandtl number Pr are the distinguishing parameters.

$$Ra = \frac{\rho_f\beta_f g L^3(T_h-T_c)}{\mu_f\alpha_f}, Pr = \frac{\mu_f}{\rho_f\alpha_f}$$

The properties of mixed nanofluid using different models in literature are grouped in Table 2.

When describing the thermo-physical characteristics of hybrid nanofluid, the volume fraction is a crucial metric. This is determined using the following formula, which takes into account the proportions of the two nanoparticle kinds distributed in the basic fluid:

$$\alpha_{hnf} = \varphi_{Al_2O_3} + \varphi_{Cu} \tag{5}$$

Table 1. The thermo-physical properties of hybrid nanofluid components [52, 55-56].

Properties	Fluid phases (water)	Al_2O_3	Cu
C_p (J/kg. K)	4179	765	383
ρ (kg/m^3)	997.1	3970	8954
k (w m^{-1} k^{-1})	0.613	40	400
β × 10^{-5}(1/k)	21	85	1.67
μ (Kg/m.s)	8.91×10^{-5}	-	-
α (m^2/s)	1.47×10^{-7}	1163.1×10^{-7}	131.7×10^{-7}

Table 2. Thermo-physical Properties

Properties	Hybrid nano-fluid	Literature studies and Model chosen
Effective density	$\rho_{hnf} = (1-\varphi_2)\left[(1-\varphi_1)\rho_f + \varphi_1\rho_{s1}\right] + \varphi_2\rho_{s2}$	[58-60]
Effective thermal expansion coefficient	$\beta_{hnf} = (1-\varphi_2)\left[(1-\varphi_1)\beta_f + \varphi_1\beta_{s1}\right] + \varphi_2\beta_{s2}$	[58-60]
Effective heat capacity	$(\rho c_p)_{hnf} = (1-\varphi_2)\left[(1-\varphi_1)(\rho c_p)_f + \varphi_1(\rho c_p)_{s1}\right] + \varphi_2(\rho c_p)_{s2}$	[58-60]
Effective thermal diffusivity	$\alpha_{hnf} = \dfrac{k_{hnf}}{(\rho c_p)_{hnf}}$	[58–60]
Effective dynamic viscosity	$\mu_{hnf} = \dfrac{\mu_f}{(1-\varphi_1)^{2.5}(1-\varphi_2)^{2.5}}$	Brinkmann Model [61]
Effective thermal conductivity	$\dfrac{k_{hnf}}{k_f}\left[\dfrac{\left(\begin{array}{c}\dfrac{(\varphi_1 k_{s1}+\varphi_2 k_{s2})}{\varphi}+2k_f\\ +2(\varphi_1 k_{s1}+\varphi_2 k_{s2})-2\varphi k_f\end{array}\right)}{\left(\begin{array}{c}\dfrac{(\varphi_1 k_{s1}+\varphi_2 k_{s2})}{\varphi}+2k_f\\ -(\varphi_1 k_{s1}+\varphi_2 k_{s2})+\varphi k_f\end{array}\right)}\right]$	Maxwell Model [62]

Table 3. Dimensionless boundary conditions

Distinct walls	Inclined wall	Bottom wall and heat source	Upright wall
Boundary conditions	$T^*=1$, $u^* = v^* = 0$	$T^*=0$, $u^* = v^* = 0$	$\dfrac{\partial T^*}{\partial x^*} = 0$, $u^* = v^* = 0$

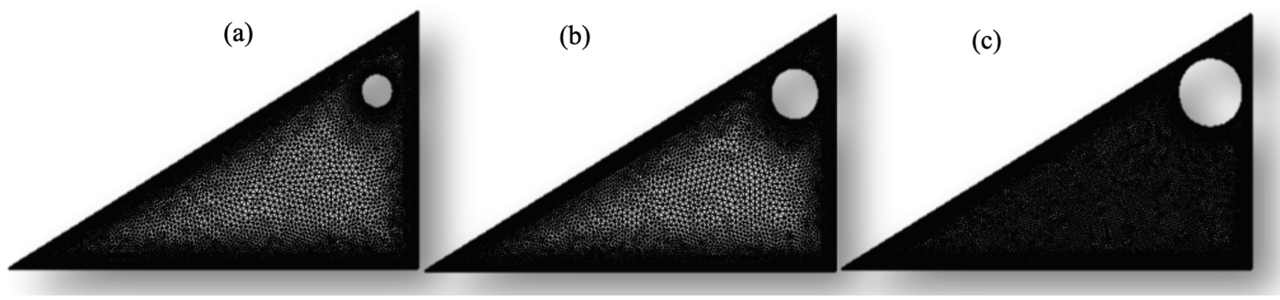

Figure 3. Optimal mesh for: (a) S_L=0.04, (b) S_L=0.06 and (c) S_L=0.08.

The dimensionless temperature and velocity boundary conditions to the enclosure as shown in Figure 1 are grouped in Table 3.

The Nusselt number relations at the tilted surface, both local and average, can be obtained using the following formulas:

$$Nu_l = -\frac{K_{hnf}}{K_f}\frac{\partial T^*}{\partial n^*} \tag{6}$$

$$Nu_{avr} = \int Nu_l dn \tag{7}$$

NUMERICAL SIMULATION AND VALIDATION CODE

Numerical Simulation

To get accurate results rapidly, verifying the solution grid dependency is necessary before drawing any conclusions on its findings. Computing the non-linear ordinary differential equations within the stated boundary conditions is done using computational grids that have been partitioned into two-dimensional spatial domains using the Galerkin FEM. Triangular elements and Lagrange-quadratic interpolation are used in this process. The finite element approach is applied to discretize

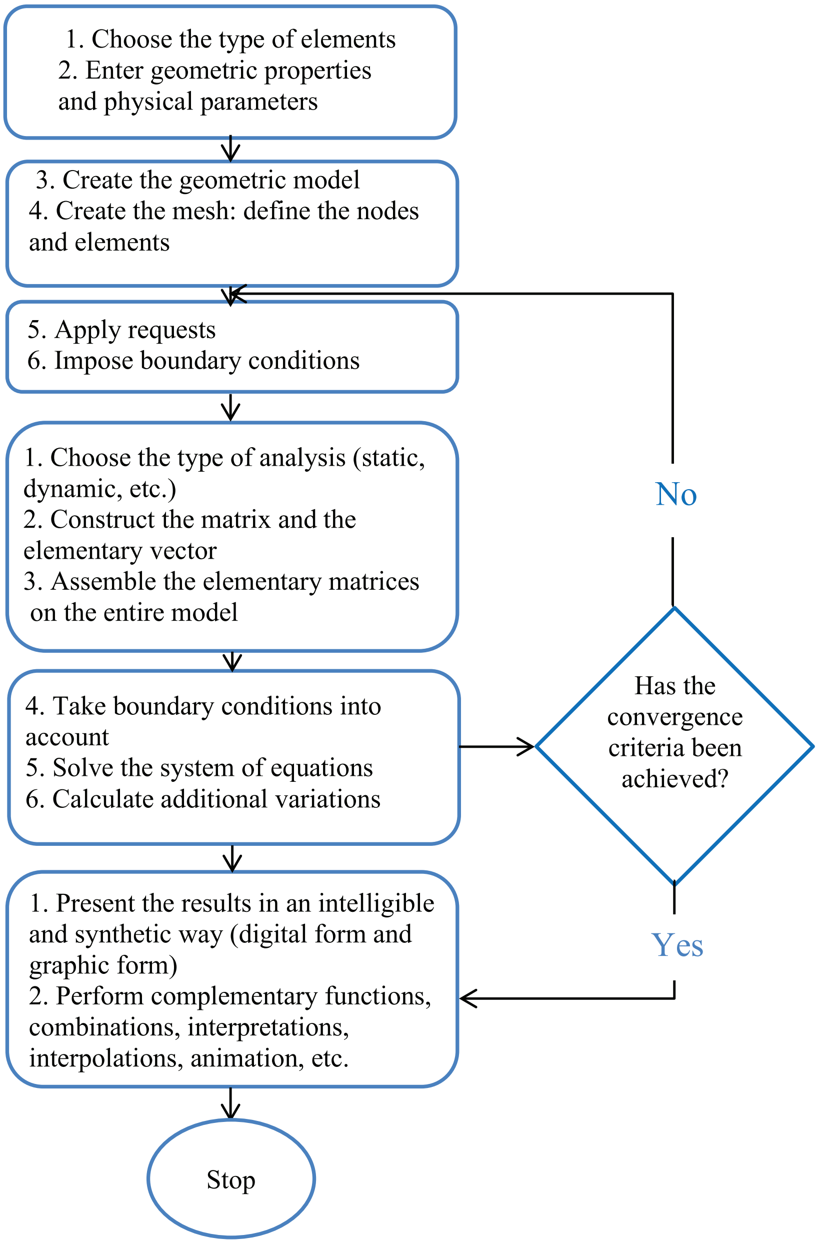

Figure 2. Analysis process using a numerical model.

Table 4. Test of mesh

Mesh	1859	2816	7145	19185	25541
Nu_{avr}	12.228	12.675	14.080	15.304	15.298

Table 5. Optimal mesh

Case	**01 (S_L=0.04)**	**02 (S_L=0.06)**	**03 (S_L=0.08)**
Boundary elements numbers	777	809	841
Domain elements numbers	19185	19269	19031

the system of mass, momentum, and energy conservation that regulate hydrodynamic and thermal flow. The velocities, temperatures, and pressures were calculated using the flowchart of finite element analysis. In order to record the temperature and velocity gradients, we fine-tuned the mesh adjacent to the boundary. The equation system yielded a solution.

This approach uses the profiles between nodes in integral computations based on differential equations integrated over the control grid. When the relative error of the supplied variables meets the following convergence requirements, we say that this approach has stable solution convergence:

$$\frac{\sum_{i=1}^{I}\sum_{j=1}^{J}\left|x_{i,j}^{m+1}-x_{i,j}^{m}\right|}{\sum_{i=1}^{I}\sum_{j=1}^{J}\left|x_{i,j}^{m+1}\right|} \leq 10^{-6} \tag{8}$$

In which i and j stand for the i^{th} and j^{th} mesh cells of the I×J structured computational domain, respectively.

The process used to analyze a physical model is shown schematically in Figure 2.

For dependable and useful outcomes, examining the grid dependency of the solution is a vital operation to do before making decisions about the findings. With S_L=0.04, Ra=10^6, and j=0.03, we averaged the Nusselt numbers of the inclined walls for several meshes in order to accomplish this. Table 4 gives the mesh test of our problem. We notice that the average Nusselt number stabilizes from grid 19185.

The different optimal meshes for the three cases, S_L=0.04, S_L=0.06 and S_L=0.08 of the problem, are summarized in Table 5 and Figures 3(a), 3(b) and 3(c). In case 01, we used a mesh of 19185 domain elements and 777 boundary layer elements.

Validation Code

The graphical results of Keramat et al.'s [63] have been compared with the current results. A cavity in the form of an H-shaped, filled with a nanofluid, is considered for this purpose. Both the highest and lowest walls are actually heated. The remaining surfaces are insulated, whereas the two vertical walls stay cold. For varying Rayleigh numbers, we found the Nu_{avr} as a function of φ of nanofluid. Our findings for the values of the Rayleigh number 10^5 and 10^6 agree well with those of Keramet, as can be seen in Figure 4. A margin of error of less than 4% is displayed in the results. Because the two authors used different numerical methods,

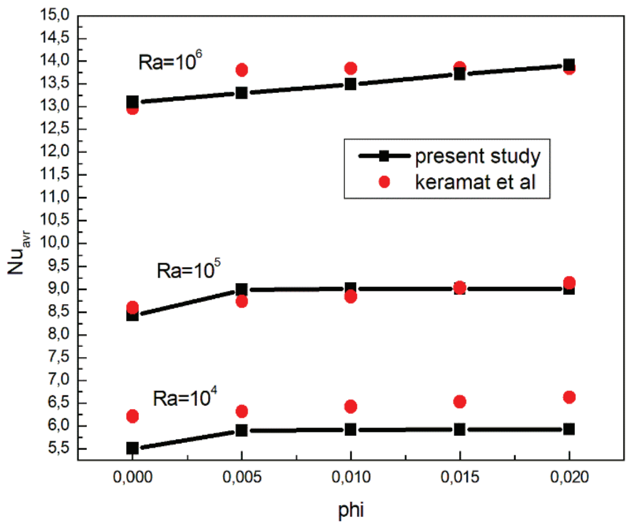

Figure 4. Validation of numerical code for average Nusselt number.

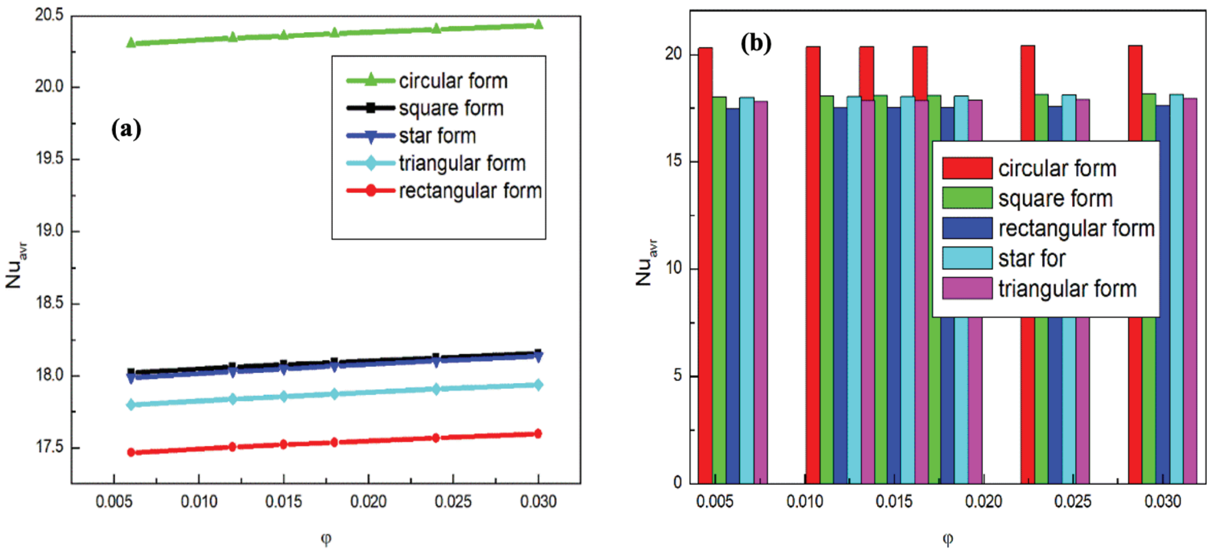

Figure 5. Average Nusselt evolution (a) and the histogram (b) at Ra=10^6 for various cold sources as a function of nanoparticle volume percentage.

there is a 10% discrepancy between the 0 and 2% fractions for the Rayleigh number $Ra=10^4$.

RESULT AND DISCUSSION

Isothermal patterns, streamlines, Nusselt numbers, and temperature fluctuations will all be presented here as findings for the three cases that were investigated. For a Rayleigh number of 10^6, we offer calculations regarding an interval of nanoparticle portions values, from 0 to 0.03.

A variety of geometric shapes, including square, circular, triangular, rectangular, and star, as well as the influence dimension, are investigated.

Influence of Cold Source Geometry on Mean Nusselt Number

For different cold source geometries, Figures 5(a) and 5(b) show the variation of Nu_{avr} and its histogram as a function of the nanoparticle fraction, respectively. We see that Nusselt's values grow to the concentration of nanoparticles in the fluid influencing all forms. We find that compared to the other shapes, the cylindrical source allows a far higher convective transfer. As an example, when we compare the geometric shapes of cylinders and rectangles for a fraction of 0.05, we see a convective regime increase of about 14%, which is great for cooling the solar panel absorber. Consequently, the most efficient and effective design for the panel is a cylindrical one, which allows for the reduction of pressure losses. Our observations are validated by the histogram.

Streamlines and Isotherms for Different Nanoparticles Fraction

For different percentages of nanoparticle volume and Ra values, Figures 6 and 7 show the dispersion of the stream function (6.a), (7.a) and isotherms (6.b), (7.b) of circular and square shapes respectively. As the nanoparticle concentrations vary, the streamline distribution (Figure 6.a) is always defined by a central cell that rotates clockwise and has a vortex at its center, which grows stronger. The strength of the convective regime's flow is amplified by this amplification. A thermal boundary layer at the inclined wall and thermal stratification on the lower portion of the panel are always features of the isothermal field distribution, which we also remark (Figure 6.b). An increment in convective transfer and a reduction in thermal conductivity of the hybrid nanofluid are both made feasible by the impact of changing the nanoparticle volume fractions on the thermal field and velocity field values.

The structure is maintained in Figure 7.a's streamlines for the square shape, with the exception that the vortex is smaller compared to the circular shape. This indicates that the convective mode flow is becoming weaker. Additionally, tiny cells have emerged, indicating the presence of load losses. Compared to Figure (6.b), Figure 7.b exhibits a broader boundary layer and substantial thermal stratification.

Therefore, a pseudo-conductive regime becomes dominant. The findings demonstrate that heat evacuation is enhanced by adjusting the concentration of the nanoparticles in the hybrid nanofluid, which impacts its thermal performance Figure (7.a). Contrasting the two shapes, we find that the square one has a wider boundary layer and a smaller vortex, suggesting that the convective transfer mode is more advantageous in the circular one. The circular shape is used for a number of reasons, including:

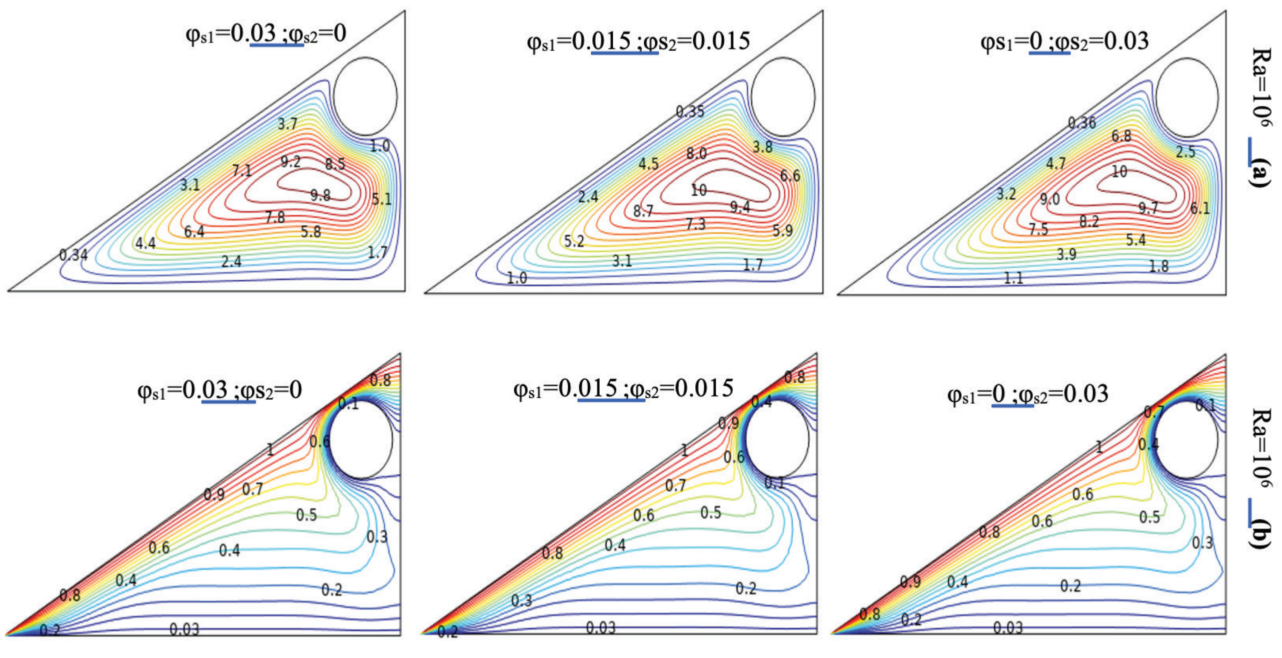

Figure 6. Streamlines (a) and Isotherms (b) of circular shape of numerous nanoparticles volume fraction for $Ra=10^6$.

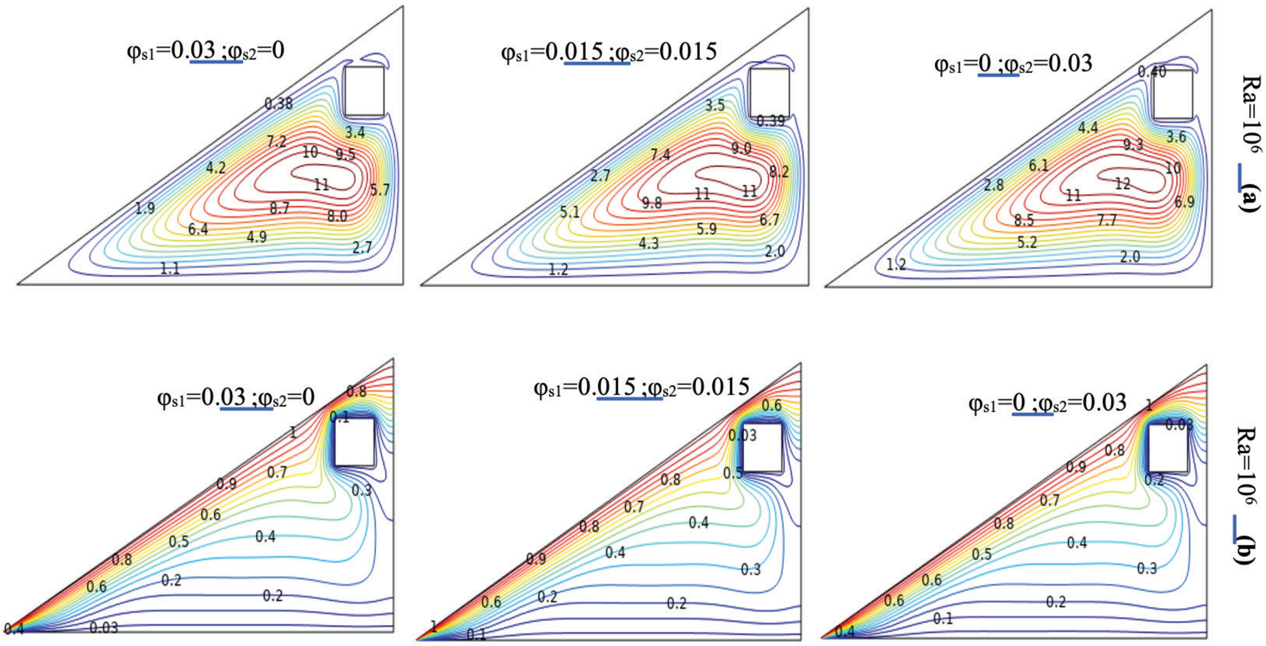

Figure 7. Streamlines (a) and Isotherms (b) of square shape of numerous nanoparticles volume fraction for Ra=10^6.

1. To prevent pressure losses and fluid shearing
2. It is easy to construct the design

Streamlines and Isotherms for Different Cold Cylinder Size

With Ra and volume fraction held constant, Figure 8 illustrates how the circulation (8.a) and thermal changes (8.b) are affected through the cold generating cylinder dimensions. Isotherms are defined by a thermal boundary layer along the slanted top wall, which stands in for the absorber, and thermal stratifications on the lower half of the panel, which provide a pseudo-conductive transmission

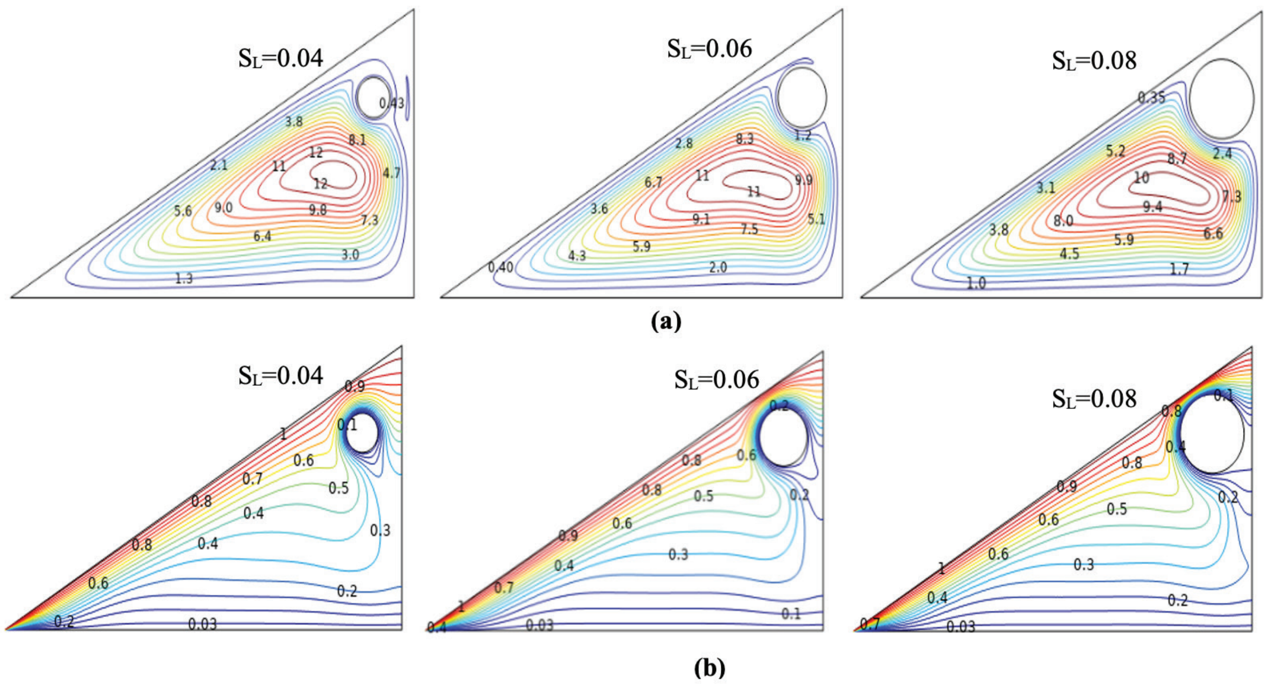

Figure 8. Streamlines (a) and Isotherms (b) of different cold source sizes for Ra=10^6 and j_{hnf}=3%.

mode. As the S_L ratio increases, the boundary layer gets narrower, which is good news for the convective transfer mode up top. A huge vortex-filled center convective cell defines the streamline distribution, and its size grows in relation to the S_L ratio. Consistent with this distribution, the convective flow regime is favored in the enclosure's central region as the S_L aspect ratio of the cylindrical source grows, leading to an intensification of the flow. The transfer mode and flow regime of the panel are directly affected by an increase in the aspect ratio of the cylindrical source S_L, as we may deduce in the conclusion.

Distribution of Temperature Along the Cold Generating Cylinder

Figure 9 displays the temperature range for S_L = 0.04, 0.06, and 0.08, φ = 0.03 and Ra = 10^6, as well as the position of the line below the cold source. As we get closer to the cool source, the temperature drops in all three cases. While there is a small fall in temperature between 0 and 0.3 m, the decrease is substantial between 0.3 and 0.5 m, particularly for a source size of S_L=0.08. This indicates that the fluid is being accelerated, leading to better evacuation of the convective mode in this region. Looking at the final temperature values across all three dimensions, we find that the temperature drops by 50% between S_L=0.08 and S_L=0.04, and by 16.67% between S_L=0.08 and S_L=0.06.

This suggests that our solar panel cooling is improving, but only to a certain extent, and that we must incorporate ventilation into our system immediately.

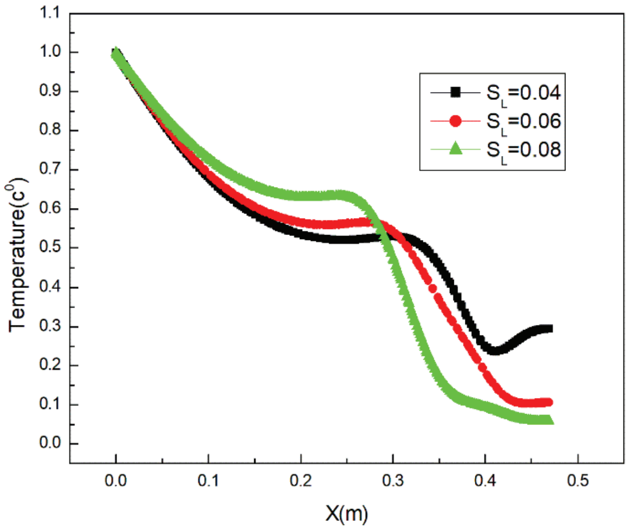

Figure 9. Temperature distribution near the lowest point of the cold source for Ra=10^6.

Solar Panel Temperature

Figure 10 illustrates the temperature distribution along the solar panel without the presence of the cold generating cylinder (10.a) and with the source (10.b) for Ra=10^6. The temperature grows at an exponential rate, as seen in Figure 10.a. Clearly, the vast upper portion of the panel is un-irradiated. As we see with natural convection, the fluid settles to the top of the panel as heat rises and cold falls. The cooling of the panel is impeded by this. Adding a cold source causes a temperature drop in a tiny top section of the panel, as shown in figure 10.b. Therefore, the fluid's flow was enhanced by the source's presence. To get the most out of the convective mode of evacuation, it is crucial to do an optimization study on the source size.

Evolution of Nuav as Function as Ra and j

Figure 11 shows that critical parameters for heat transfer include the number of Rayleigh and the nanofluid volume portions. Ra sees the increasing trend of the Nuavr rises in

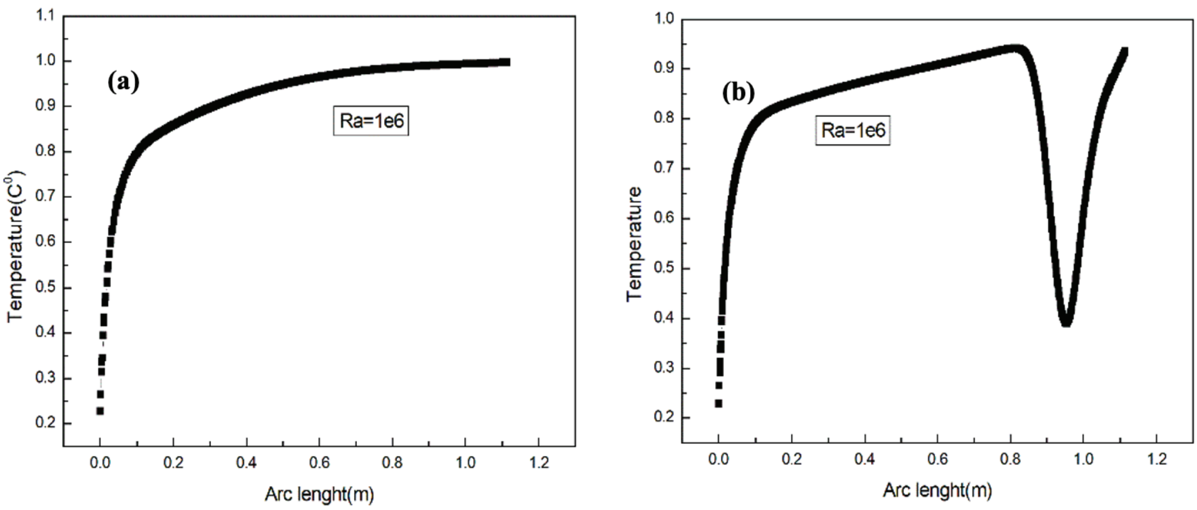

Figure 10. Temperature distribution along the solar panel without the cold generating cylinder (a) and with the presence of the cold generating cylinder (b) for Ra=10^6.

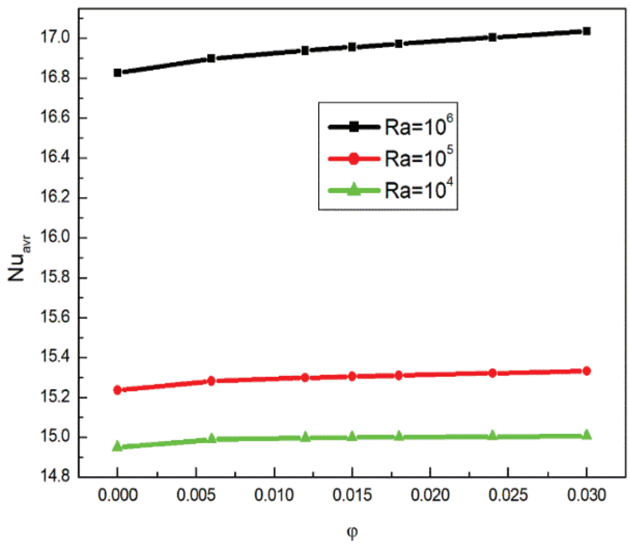

Figure 11. Nu_{avr} at different Ra and nanoparticles volume fraction for circular form.

all curves. Also, heat transmission is improved when the nanofluid volume percentage is increased.

The enhanced heat transfer is the reason behind the change in fluid properties caused by injecting of Al_2O_3 and Cu nanoparticles directly into water.

Variation of Nuav as Function as SL

The average Nusselt number plotted against the magnitude of the cold cylinder is shown in Figure 12 for $Ra=10^6$ and $\varphi=0.03$. As the heat source dimension improves, numerical simulations disclose the fact that both convective heat transport and Nusselt values increase.

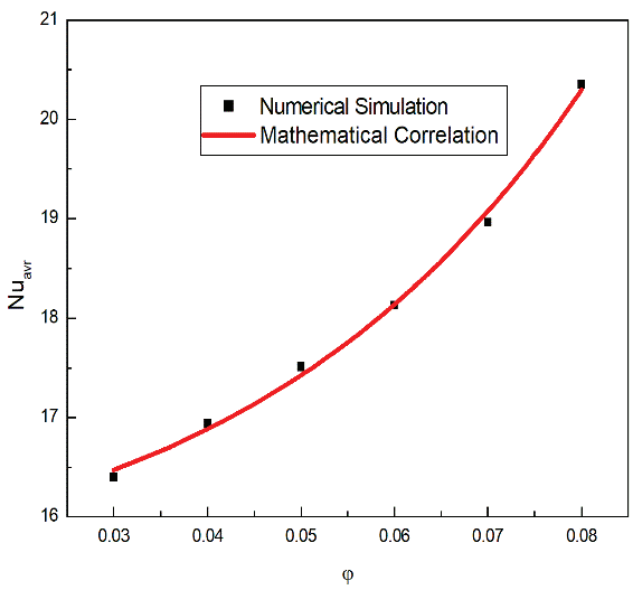

Figure 12. The cold source's size affects the Nu_{avr}.

As the regression coefficient indicates $R^2=0.99$, the mathematical correlation requires on an exponential form.

$$Nu_{avr} = 15.208 + 0.554e^{\left(\frac{S_L}{0.036}\right)}$$

CONCLUSION

This research investigates how the size and geometry of cold cylinder impacts the hydrodynamic and thermal flow in a triangular cavity full of hybrid nanofluid, aiming to optimize cooling conditions for solar panels. The results obtained in isothermal form, streamline, mean Nusselt number and temperature profile at various Rayleigh values; allow us to deduce the following points:

- o Raising the volume fraction concentrations of nanoparticles in water enhances the convective transfer regime, while increasing the aspect ratio intensifies the flow.
- o As the aspect ratio increases, solar panel cooling becomes more dependable.
- o A rise in the Rayleigh number and the volume percentage of the nanoparticles enhances the average Nusselt evolution, which grows exponentially with the cold generating cylinder size.
- o An ideal cold source would have a cylindrical shape with an aspect ratio of $S_L=0.08$, which would greatly improve the efficiency and performance of the solar panel.

Considering the thermal stratification of the hybrid nanofluid, our analysis indicates that the majority of our solar panels lack sufficient cooling. This does not bode well for our semi-arid climate. This is why we're going to build ventilation to improve our cooling system.

NOMENCLATURE

Ra	Rayleigh number
Pr	Prandtl Number
Nu	Nusselt number
G	Gravitational acceleration, $m.s^{-2}$
x, y	Cartesian coordinates, m
P	Pressure, $N.m^{-2}$
T	Temperature [K]
K	Thermal conductivity, $W.m^{-1}.K^{-1}$
u,v	Components of velocity fields, $m.s^{-1}$
X*,y*	Dimensionless coordinates, m
u*,v*	Dimensionless velocity components, $m.s^{-1}$
P*	Dimensionless pressure
S_L	The coled source size
H	Height of cavity
L	Base of cavity
H_s	source's height

Greec Symbol

A	Thermal diffusivity, $m^{-2}.s^{-1}$
B	Coefficient of thermal expansion, K^{-1}

μ	Dynamic viscosity, $kg.m^{-1}.s^{-1}$
Ρ	Density, $kg.m^{-3}$
(ρC_p)	Heat capacity, $J.m^{-3}.K^{-1}$
j	Volume fraction

Subscripts

f	Fluid properties
hnf	Hybrid nanofluid properties
s	Solid properties
c	Cold wall
h	Hot wall
eff	Effective
*	Dimensional properties
avr	Average
FEM	Finite element method
L	Local

AUTHORSHIP CONTRIBUTIONS

Authors equally contributed to this work.

DATA AVAILABILITY STATEMENT

The authors confirm that the data that supports the findings of this study are available within the article. Raw data that support the finding of this study are available from the corresponding author, upon reasonable request.

CONFLICT OF INTEREST

The author declared no potential conflicts of interest with respect to the research, authorship, and/or publication of this article.

ETHICS

There are no ethical issues with the publication of this manuscript.

STATEMENT ON THE USE OF ARTIFICIAL INTELLIGENCE

Artificial intelligence was not used in the preparation of the article.

REFERENCES

[1] Kaushik SC, Verma A, Tyagi SK. Advances in solar absorption cooling systems: An overview. J Therm Eng 2024;10:1044–1067. [CrossRef]
[2] Sharma DK, Rathod MK, Bhale PV. Enhancement in thermal and electrical characteristics of solar photovoltaic module through a direct contact water jacketed cooling system. J Therm Eng 2021;10:360–374. [CrossRef]
[3] Djermane K, Kadri S. Computational study of crossed-cavity hybrid nanofluid turbulent forced convection for enhanced concentrated solar panel cooling. J Nanofluids 2023;12:1895–1902. [CrossRef]
[4] Komeili Birjandi A, Eftekhari Yazdi M, Dinarvand S, Salehi GR, Tehrani P. Effect of using hybrid nanofluid in thermal management of photovoltaic panel in hot climates. Int J Photoenergy 2021;1:3167856. [CrossRef]
[5] Natarajan R, Gaikwad PR, Basil E, Borse SD. Heat enhancement in solar flat plate collectors–A review. J Therm Eng 2024;10:773–789. [CrossRef]
[6] Shahini N, Karami M, Behabadi MAA. Numerical investigation of direct absorption evacuated tube solar collector using alumina nanofluid. J Therm Eng 2021;10:562–571. [CrossRef]
[7] Hussein AM, Awad AT, Ali HHM. Evaluation of the thermal efficiency of nanofluid flows in flat plate solar collector. J Therm Eng 2024;10:299–307. [CrossRef]
[8] Liu GL, Liu J. Convective cooling of compact electronic devices via liquid metals with low melting points. J Heat Transf 2021;143:050801. [CrossRef]
[9] Aminossadati SM, Ghasemi B. Natural convection cooling of a localised heat source at the bottom of a nanofluid-filled enclosure. Eur J Mech B Fluids 2009;28:630–640. [CrossRef]
[10] Lam PAK, Prakash KA. A numerical study on natural convection and entropy generation in a porous enclosure with heat sources. Int J Heat Mass Transf 2014;69:390–407. [CrossRef]
[11] Mobedi M, Sunden B. Natural convection heat transfer from a thermal heat source located in a vertical plate fin. Int Commun Heat Mass Transf 2006;33:943–950. [CrossRef]
[12] El Moutaouakil L, Boukendil M, Hidki R, Charqui Z, Zrikem Z, Abdelbaki A. Analytical solution for natural convection of a heat-generating fluid in a vertical rectangular cavity with two pairs of heat source/sink. Therm Sci Eng Prog 2023;40:101738. [CrossRef]
[13] Mohebbi R, Izadi M, Chamkha AJ. Heat source location and natural convection in a C-shaped enclosure saturated by a nanofluid. Phys Fluids 2017;29:122009. [CrossRef]
[14] Njoroge J, Gao P. Enhanced cooling of a localized heat source by natural convection in an annular channel. In: Proc Int Conf Nucl Eng (ICONE) 2023;30:1352. [CrossRef]
[15] Daghab H, Kaddiri M, Raghay S, Arroub I, Lamsaadi M, Rayhane H. Finite volume simulation of natural convection for power-law fluids with temperature-dependent viscosity in a square cavity with a localized heat source. Int J Heat Technol 2021;39:1405–1416. [CrossRef]
[16] Ibrahim M, Saeed T, Algehyne EA, Alsulami H, Chu YM. Optimization and effect of wall conduction on natural convection in a cavity with constant temperature heat source: Using lattice Boltzmann method and neural network algorithm. J Therm Anal Calorim 2021;144:2449–2463. [CrossRef]

[17] Gangawane KM, Bharti RP, Kumar S. Effects of heating location and size on natural convection in partially heated open-ended enclosure by using lattice Boltzmann method. Heat Transf Eng 2016;37:507–522. [CrossRef]

[18] Choudhary R, Subudhi S. Aspect ratio dependence of turbulent natural convection in Al_2O_3/water nanofluids. Appl Therm Eng 2016;108:1095–1104. [CrossRef]

[19] Ghodsinezhad H, Sharifpur M, Meyer JP. Experimental investigation on cavity flow natural convection of Al_2O_3–water nanofluids. Int Commun Heat Mass Transf 2016;76:316–324. [CrossRef]

[20] Sharifpur M, Solomon AB, Ottermann TL, Meyer JP. Optimum concentration of nanofluids for heat transfer enhancement under cavity flow natural convection with TiO_2–water. Int Commun Heat Mass Transf 2018;98:297–303. [CrossRef]

[21] Rao PS, Barman P. Natural convection in a wavy porous cavity subjected to a partial heat source. Int Commun Heat Mass Transf 2021;120:105007. [CrossRef]

[22] Sankar M, Park J, Kim D, Do Y. Numerical study of natural convection in a vertical porous annulus with an internal heat source: Effect of discrete heating. Numer Heat Transf A Appl 2013;63:687–712. [CrossRef]

[23] Dogonchi AS, Nayak MK, Karimi N, Chamkha AJ, Ganji DD. Numerical simulation of hydrothermal features of Cu–H_2O nanofluid natural convection within a porous annulus considering diverse configurations of heater. J Therm Anal Calorim 2020;141:2109–2125. [CrossRef]

[24] Belhocine A, Abdullah OI. Comparative study of two numerical methods for solving the Graetz problem: The orthogonal collocation and Crank-Nicholson methods. Lat Am Appl Res 2016;73–79. [CrossRef]

[25] Manh TD, Abazari AM, Barzegar Gerdroodbary M, Nam ND, Moradi R, Babazadeh H. Computational simulation of variable magnetic force on heat characteristics of backward-facing step flow. J Therm Anal Calorim 2021;144:1585–1596. [CrossRef]

[26] Belhocine A, Omar WZW. Analytical solution and numerical simulation of the generalized Levèque equation to predict the thermal boundary layer. Math Comput Simul 2021;180:43–60. [CrossRef]

[27] Belhocine A, Abdullah OI. Numerical simulation of thermally developing turbulent flow through a cylindrical tube. Int J Adv Manuf Technol 2019;102:2001–2012. [CrossRef]

[28] Belhocine A, Omar WW. Numerical study of heat convective mass transfer in a fully developed laminar flow with constant wall temperature. Case Stud Therm Eng 2015;6:116–127. [CrossRef]

[29] Afzal A, Soudagar MEM, Belhocine A, Kareemullah M, Hossain N, Alshahrani S, et al. Thermal performance of compression ignition engine using high content biodiesels: A comparative study with diesel fuel. Sustainability 2021;13:7688. [CrossRef]

[30] Madhi H, Aljabair S, Imran AA. A review of photovoltaic/thermal system cooled using mono and hybrid nanofluids. Int J Thermofluids 2024;22:100679. [CrossRef]

[31] Kaplan S, Bayramoğlu K, Sarıkanat M, Altay L. Numerical study on heat transfer and fluid dynamics in plate heat exchangers: Effects of chevron angle and aspect ratio. J Therm Eng 2024;638–656. [CrossRef]

[32] Tlili I, Moradi R, Barzegar Gerdroodbary M. Transient nanofluid squeezing cooling process using aluminum oxide nanoparticle. Int J Mod Phys C 2019;30:1950078. [CrossRef]

[33] Manh TD, Bahramkhoo M, Barzegar Gerdroodbary M, Nam ND, Tlili I. Investigation of nanomaterial flow through non-parallel plates. J Therm Anal Calorim 2021;143:3867–3875. [CrossRef]

[34] Barzegar Gerdroodbary M. Application of neural network on heat transfer enhancement of magnetohydrodynamic nanofluid. Heat Transf Asian Res 2020;49:197–212. [CrossRef]

[35] Kumararaja K, Sıvaraman B, Saravanan S. Performance evaluation of hybrid nanofluid-filled cylindrical heat pipe by machine learning algorithms. J Therm Eng 2024;10:286–298. [CrossRef]

[36] Rashad AM, Chamkha AJ, Ismael MA, Salah T. Magnetohydrodynamics natural convection in a triangular cavity filled with a Cu-Al_2O_3/water hybrid nanofluid with localized heating from below and internal heat generation. J Heat Transf 2018;140:072502. [CrossRef]

[37] Manjunatha S, Kuttan BA, Jayanthi S, Chamkha A, Gireesha BJ. Heat transfer enhancement in the boundary layer flow of hybrid nanofluids due to variable viscosity and natural convection. Heliyon 2019;5:e01469. [CrossRef]

[38] Selimefendigil F, Chamkha AJ. Natural convection of a hybrid nanofluid-filled triangular annulus with an opening. Comput Therm Sci 2016;8:555–566. [CrossRef]

[39] Alsabery AI, Kadhim HT, Ismael MA, Hashim I, Chamkha AJ. Impacts of amplitude and heat source on natural convection of hybrid nanofluids into a wavy enclosure via heatline approach. Waves Random Complex Media 2023;33:1060–1084. [CrossRef]

[40] Hachichi F, Belghar N, Kamel C, Saleh MS, Kadja M, Lachi M, et al. Obstacle's effects and their location inside the square cavity on the thermal performance of Cu–Al_2O_3/H_2O hybrid nanofluid. Heat Transf 2023;52:3411–3430. [CrossRef]

[41] Wang Y, Chen J, Zhang W. Natural convection in a circular enclosure with an internal cylinder of regular polygon geometry. AIP Adv 2019;9:065023. [CrossRef]
[42] Roy NC. Natural convection of nanofluids in a square enclosure with different shapes of inner geometry. Phys Fluids 2018;30:113605. [CrossRef]
[43] Tayebi T, Chamkha AJ. Effects of various configurations of an inserted corrugated conductive cylinder on MHD natural convection in a hybrid nanofluid-filled square domain. J Therm Anal Calorim 2021;143:1399−1411. [CrossRef]
[44] Acharya N. On the flow patterns and thermal behaviour of hybrid nanofluid flow inside a microchannel in presence of radiative solar energy. J Therm Anal Calorim 2020;141:1425−1442. [CrossRef]
[45] Chadi K, Battira MM, Saleh MS, Belghar N, Lachi M, Chamkha AJ. Impact of geometric shape of cavity on heat exchange using Cu-Al_2O_3-H_2O hybrid nanofluid. Waves Random Complex Media 2022;1−18. [CrossRef]
[46] Hidki R, El Moutaouakil L, Charqui Z, Boukendil M, Zrikem Z. Natural convection in a square cavity containing two heat-generating cylinders with different geometries. Mater Today Proc 2021;45:7415−7423. [CrossRef]
[47] Pandey S, Park YG, Ha MY. An exhaustive review of studies on natural convection in enclosures with and without internal bodies of various shapes. Int J Heat Mass Transf 2019;138:762−795. [CrossRef]
[48] Mourad A, Aissa A, Mebarek-Oudina F, Jamshed W, Ahmed W, Ali HM, et al. Galerkin finite element analysis of thermal aspects of Fe_3O_4-MWCNT/water hybrid nanofluid filled in wavy enclosure with uniform magnetic field effect. Int Commun Heat Mass Transf 2021;126:105461. [CrossRef]
[49] Revnic C, Groşan T, Sheremet M, Pop I. Numerical simulation of MHD natural convection flow in a wavy cavity filled by a hybrid Cu-Al_2O_3-water nanofluid with discrete heating. Appl Math Mech 2020;41:1345−1358. [CrossRef]
[50] Izadi M, Mohebbi R, Karimi D, Sheremet MA. Numerical simulation of natural convection heat transfer inside a⊥ shaped cavity filled by a MWCNT-Fe3O4/water hybrid nanofluids using LBM. Chem Eng Process Process Intensif 2018;125:56−66. [CrossRef]
[51] Alomari MA, Al-Farhany K, Hashem AL, Al-Dawody MF, Redouane F, Olayemi OA. Numerical study of MHD natural convection in trapezoidal enclosure filled with (50% MgO-50% Ag/water) hybrid nanofluid: Heated sinusoidal from below. Int J Heat Technol 2021;39:1271−1279. [CrossRef]
[52] Chamkha AJ, Miroshnichenko IV, Sheremet MA. Numerical analysis of unsteady conjugate natural convection of hybrid water-based nanofluid in a semicircular cavity. J Therm Sci Eng Appl 2017;9:041004. [CrossRef]
[53] Pordanjani AH, Aghakhani S. Numerical investigation of natural convection and irreversibilities between two inclined concentric cylinders in presence of uniform magnetic field and radiation. Heat Transf Eng 2022;43:937−957. [CrossRef]
[54] Astanina MS, Sheremet MA. Numerical study of natural convection of fluid with temperature-dependent viscosity inside a porous cube under non-uniform heating using local thermal non-equilibrium approach. Int J Thermofluids 2023;17:100266. [CrossRef]
[55] Ben Hamida MB, Charrada K. Natural convection heat transfer in an enclosure filled with an ethylene glycol-copper nanofluid under magnetic fields. Numer Heat Transf A Appl 2015;67:902−920. [CrossRef]
[56] Gupta M, Singh V, Kumar S, Kumar S, Dilbaghi N, Said Z. Up to date review on the synthesis and thermophysical properties of hybrid nanofluids. J Clean Prod 2018;190:169−192. [CrossRef]
[57] Colin S. International journal of heat and technology: Foreword. Int J Heat Technol 2008;26:107.
[58] Hamilton RL, Crosser OK. Thermal conductivity of heterogeneous two-component systems. Ind Eng Chem Fundam 1962;1:187−191. [CrossRef]
[59] Keramat F, Dehghan P, Mofarahi M, Lee CH. Numerical analysis of natural convection of alumina−water nanofluid in H-shaped enclosure with a V-shaped baffle. J Taiwan Inst Chem Eng 2020;111:63−72. [CrossRef]
[60] Ali K, Ahmad S, Tayebi T, Ashraf M, Jamshed W, Abd-Elmonem A, et al. Thermal attributes of hybrid (MWCNT-NiZnFe2O4) nanofluid flow having motile microbes and activation energy: A computational approach. Case Stud Therm Eng 2023;47:103088. [CrossRef]
[61] Maxwell JC. A treatise on electricity and magnetism. Vol. 1. Oxford: Clarendon Press; 1873.
[62] Brinkman HC. The viscosity of concentrated suspensions and solutions. J Chem Phys 1952;20:571. [CrossRef]
[63] Keramat F, Dehghan P, Mofarahi M, Lee CH. Numerical analysis of natural convection of alumina−water nanofluid in H-shaped enclosure with a V-shaped baffle. J Taiwan Inst Chem Eng 2020;111:63−72. [CrossRef]